Journal of Luminescence 47 (1990) 113–127
North-Holland

Auger ionization of semiconductor quantum drops in a glass matrix

D.I. Chepic, Al.L. Efros, A.I. Ekimov, M.G. Ivanov, V.A. Kharchenko, I.A. Kudriavtsev and T.V. Yazeva

A.F. Ioffe Physico-Technical Institute, 194021 Leningrad, USSR

Received 1 October 1989
Revised 23 April 1990
Accepted 26 April 1990

A microscopic model of degradation of both the nonlinear optical and luminescent properties of semiconductor-doped glasses is proposed. In the framework of the model the degradation is due to the process of Auger ionization of microcrystals when some electron–hole pairs are excited. The theoretical dependences of Auger ionization rate on the microcrystal size and energy band parameters of the glass/semiconductor heterostructures are obtained. The luminescence degradation kinetics have been studied in CdS microcrystal doped glasses with different average size at various pumping light intensities. The experimental dependences of the ionization rate on the microcrystal size and intensity are found to be in good agreement with the theoretical calculations. It is shown that an abrupt heterointerface leads to a strong increase of the Auger process rate. Oscillations of the Auger ionization probability and their dependences on the microcrystal size are predicted.

1. Introduction

Optical properties of semiconductor microcrystals with quantum size-governed spectra have been receiving considerable attention recently [1–5]. It is connected with the possibility to change optical properties in a controlled manner [1–6], since the variation of the size of much microcrystals (the so-called 'quantum drops') leads to the modification of energy spectra of the intrinsic [5,6] and impurity [7] states.

The important peculiarity of quantum drops dispersed in a glass matrix is a substantial nonlinearity of their optical properties [8,9]. However, degradation of the luminescent and nonlinear properties, which occurs under illumination, limits the application of these structures. This effect was shown [11,12] to be due to ionization of microcrystals by optical photon excitation, followed by the capture of the ejected electron by long-lived centers in the glass [11,12]. The purpose of this paper is to clarify the microscopic nature of the microcrystal ionization resulting in the degradation of their optical properties.

Consider this phenomenon qualitatively. The energy of optical photons is smaller than the energy of direct ejection of the electrons from the microcrystal. Therefore, the main source of ionization of microcrystals must be Auger annihilation of nonequilibrium electron–hole pairs, which are created in the microcrystal as a result of absorption of more than two photons. The charged microcrystals which appear as a result of such Auger-ionization exhibit a low quantum efficiency*. It leads to the degradation of the optical properties of these semiconductor structures. The rate of the degradation processes is determined

* The observed enhancement of the nonradiative channel can be a result of effective Auger-recombination in charged microcrystals since three quasiparticles (one electron and two holes) are formed when only one electron–hole pair is photoexcited. The charge state of a microcrystal does not change if the energy obtained by the hole as a result of this Auger recombination is insufficient to eject it from the microcrystal. This means that the band offset has to be larger for the valence band than for the conduction band.

by the Auger ionization rate and the probability of creation of two electron–hole pairs in the microcrystal under illumination.

The interimpurity luminescence data, which include the degradation rates measured in microcrystals of different size at various photoexcitation intensities and their characteristic ionization times, are presented in the second section of the paper.

Sections 3 and 4 are devoted to the theoretical consideration of the dependence of the Auger ionization rate on the size of microcrystals and on the energy band parameters. In the last section the experimental data are compared to the theoretical calculation and the results are discussed.

2. Experimental results

In this paper we investigated the kinetics of photoluminescence degradation in CdS microcrystals grown in a silicate glass matrix by the technology described in ref. [13]. The values of the average radius of microcrystals $\bar{a}$ were measured for each sample by the method of small angle X-ray scattering in the approximation of spherical particles and were accordingly $\bar{a} = 13$, 16, 22, 33 and 39 Å. Photoluminescence measurements were made at temperature $T = 77$ K.

The absorption spectra of the investigated samples are shown in fig. 1. A shift of the band edge to shorter wavelengths and oscillations in the interband absorption spectra are observed with decreasing microcrystal size which, as was shown earlier [14], is due to the size quantization of electrons in the conduction band. The arrows in fig. 1 show the spectral positions of the krypton laser lines $\lambda = 406$ and $\lambda = 476$ nm. The line $\lambda = 406$ nm is used for photoluminescence excitation in all investigated samples. The line $\lambda = 476$ nm is used for examination of the dependence of the degradation rate on the energy of excitation light quanta for the sample with $\bar{a} = 39$ Å. Detection of photoluminescence was carried out in the range of band maximum ($D-A_2$), which is due to the transitions from the deep acceptor (binding energy $E_{A_2} = 0.9$ eV) to the donor ($E_D = 0.075$ eV) [7].

The degradation of photoluminescence intensity I_{lum}, measured on the sample with $\bar{a} = 22$ Å at different intensities of the exciting light I, is shown in fig. 2. As is seen in fig. 2, the rate of luminescence degradation and the final value of the decreased luminescence intensity depend strongly on the excitation intensity I.

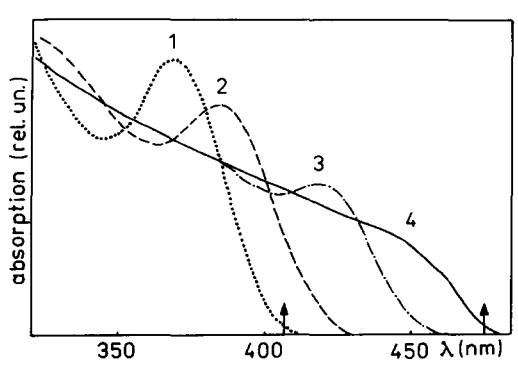

Fig. 1. Absorption spectra of CdS microcrystals with different average sizes at $T = 77$ K. 1; $\bar{a} = 13$ Å, 2; 16 Å, 3; 22 Å, 4; 39 Å.

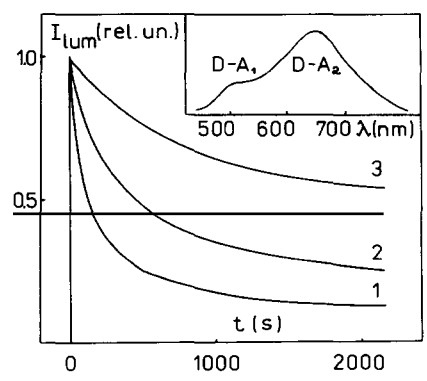

Fig. 2. The dependence of luminescence intensity I_{lum} on time at different intensity of excitation: 1; I, 2; $0.45I$, 3; $0.2I$. The inset shows the luminescence spectrum of the same sample with $\bar{a} = 22$ Å.

To describe the experimental results, we consider the simplest phenomenological model based on the competition of Auger-ionization with neutralization processes in microcrystals. Neutralization occurs as a result of the return of the electron into the microcrystals either thermally or by tunneling.

Three types of excited microcrystals exist in glass (with a total concentration of microcrystals N) under illumination: microcrystals containing one nonequilibrium electron–hole pair (N_1 is their concentration), two electron–hole pairs (N_2 is their concentration)* and ionized microcrystals with concentration N_+. The equations which describe the kinetics of the filling of excited microcrystal states have the form:

$$\begin{aligned} dN_0/dt &= -W_{01}N_0 + N_1/\tau_0^{(1)}, \\ dN_1/dt &= W_{01}N_0 - \left(W_{12} + 1/\tau_0^{(1)}\right)N_1 + N_2/\tau_0^{(2)} + N_+/\tau, \\ dN_2/dt &= W_{12}N_1 - \left(1/\tau_A + 1/\tau_0^{(2)}\right)N_2, \\ dN_+/dt &= N_2/\tau_A - N_+/\tau, \end{aligned} \tag{1}$$

where $N_0 = N - (N_1 + N_2 + N_+)$ is the concentration of nonexcited microcrystals; W_{01}, W_{12} are the probabilities of photon absorption by a nonexcited microcrystal and by microcrystals containing one electron–hole pair, respectively. τ_A^{-1} is the probability of Auger ionization in a microcrystal with two electron–hole pairs, τ is the characteristic time of neutralization, and $\tau_0^{(1,2)}$ are the lifetimes of excited states with one and two nonequilibrium electron–hole pairs, respectively. The luminescence intensity I_{lum} is proportional to the concentration of microcrystals with one electron–hole pair $N_1(t)$: $I_{lum} = \text{const} \times N_1(t)$. The microcrystals with two electron–hole pairs do not give a significant contribution to the luminescence because at the excitation intensity used in our experiment their concentration $N_2 \ll N_1$. Therefore, the process of the luminescence degradation is represented by the slow part of the time dependence $N_1(t)/N_1(0)$. The fast part of the time dependence $N_1(t)$ involves times of the order of $\tau_0^{(1,2)} \sim 10^{-9}$ s and does not reveal the degradation processes.

The system of linear equations (1) is solved by the standard technique. Assuming an exponential form of the solution with characteristic times γ^{-1} we obtain a 4th order equation for γ. At low excitation intensities I, when $W_{01}\tau_0^{(1)} \ll 1$, $W_{12}\tau_0^{(2)} \ll 1$, degradation is determined by the smallest root of this equation γ_{min}, which can be easily found neglecting the terms of order higher than γ^2. The dependence of the relative intensity of luminescence $J_{lum} = I_{lum}(t)/I_{lum}(0)$ obtained from (1) has the form:

$$\begin{aligned} J_{lum} &= \frac{N_1(t)}{N_1(0)} = \frac{\tau}{\tau_i + \tau} \exp\left[-t\left(\frac{1}{\tau} + \frac{1}{\tau_i}\right)\right] + \frac{\tau_i}{\tau_i + \tau}, \\ \gamma_{min} &= \tau_i^{-1} = \left(W_{01}\tau_0^{(1)}\right)\frac{\left(W_{12}\tau_0^{(2)}\right)}{\left(\tau_0^{(2)} + \tau_A\right)}, \end{aligned} \tag{2}$$

where τ_i is a typical time of ionization of the microcrystal. In the case of fast Auger processes, when $\tau_A \ll \tau_0^{(2)}$, the rate of ionization is determined only by the rate of creation of microcrystals with two electron–hole pairs: $\tau_i^{-1} = (W_{01}\tau_0^{(1)})W_{12}$. As will be shown in the next section the situation in which the Auger annihilation rate is less than $\tau_0^{(2)}$ is more realistic. In that case the ionization rate is equal to the probability of a microcrystal containing two electron–hole pairs, multiplied by the Auger annihilation rate:

$$\tau_i^{-1} = \left(W_{01}\tau_0^{(1)}\right)\left(W_{12}\tau_0^{(2)}\right)/\tau_A. \tag{3}$$

At low intensity of pumping light I the probability of ionization is always proportional to I^2, since probability $W \sim I$.

* Microcrystals containing more electron–hole pairs were not considered because their concentration is much smaller than N_2 at low excitation intensities I.

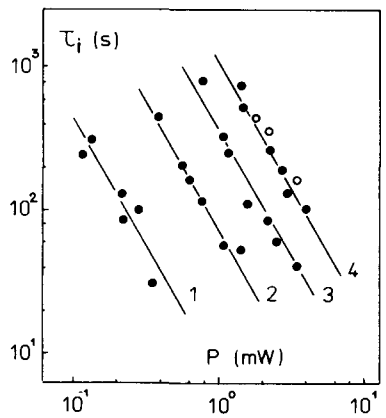

Fig. 3. The dependence of ionization time τ_i on absorption power P for microcrystals with different size. Black circles show the experimental points at excitation line $\lambda = 40$ nm and open circles at $\lambda = 476$ nm. 1; $\bar{a} = 13$ Å, 2; 16 Å, 3; 22 Å, 4; 39 Å.

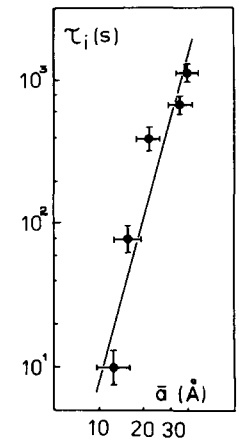

Fig. 4. The dependence of ionization time τ_i on the microcrystal size at fixed power of absorption light $P = 1$ mW.

In fig. 3 we show the experimental dependences of ionization time τ_i on the absorbed power P obtained by means of eq. (2). P is connected to the probability of light absorption $P = (W_{01}N)\hbar\omega$, where $\hbar\omega$ is the energy of absorbed photons and N is the concentration of the microcrystals participating in absorption. The curves (1–4) correspond to samples containing microcrystals with different average size $\bar{a}$. It is seen that the dependences of the ionization time τ_i on the absorbed power P have the form $\tau_i \sim P^{-\nu}$ where $\nu = 1.80 \pm 0.3$. The characteristic times of neutralization, τ, obtained from our experiments are $\sim 4.0 \times 10^2$ s, and within the experimental error of 25% they do not depend on the microcrystal size and on the intensity of exciting light.

In fig. 4 we show the experimental dependence of the ionization time on the average size of microcrystals at a fixed value of absorbed power $P = 1$ mW. It is seen that the ionization time increases strongly when $\bar{a}$ grows and this dependence has the form $\tau_i \sim (\bar{a})^{4.5}$. The dependences found reflect the parametric behavior of the Auger annihilation time since $\tau_i \sim \tau_A P^{-2} N^2$ (see eq. (3)). The discussion of that dependence will be carried out in section 5 after calculating the size dependence of the Auger ionization probability $1/\tau_A$.

3. Energy spectra and wave functions of carriers in semiconductor microcrystals dispersed in glass

The calculation of the Auger annihilation probability is a difficult problem even in the bulk semiconductor as it demands the exact calculation of the small overlap integrals of the electron–hole states [15]. Therefore, the wave functions of the electron–hole pairs of such quasi zero-dimensional structures should be considered in the many-band approximation. The second difficulty is that the electron ejection from the microcrystal (ionization) demands consideration of quantum structures with finite barrier height. Calculations taking into account the finite barrier height and many bands (which lead to a nonparabolic energy spectrum of carriers) have not been made before. In this paper we do this in the framework of a Kane model [16,17].

The basis functions of the Kane model were chosen in the form: $u_c = |S\rangle$, the Bloch function of the conduction band; $u_{m=\pm 1} = \pm(|X\rangle \pm i|Y\rangle)/\sqrt{2}$ and $u_{m=0} = |Z\rangle$, the Bloch functions of the valence band. Then the electron wave function has the form:

$$\Psi^e = \Psi_s(r)u_c + \sum_{m=-1}^{m=1} \Psi_m(r)u_{-m}, \tag{4}$$

where $\Psi_i(r)$ are envelope functions. Substituting Ψ^e in Schrödinger's equation we obtain the expressions for Ψ_m, which constitute the mixing of the valence band into the electron states:

$$\Psi_0 = -\frac{V}{E+E_g/2}\hat{p}_z\Psi_s, \qquad \Psi_{\pm 1} = \mp\frac{V}{E+E_g/2}\hat{p}_{\pm}\Psi_s, \tag{5}$$

where E is the energy of the state measured from the middle of the energy gap with width E_g, $\hat{p}_z = -i\hbar\,\partial/\partial z$, $\hat{p}_{\pm} = -i\hbar(\partial/\partial x \pm i\,\partial/\partial y)/\sqrt{2}$, $V = \langle S|\hat{p}_z|Z\rangle/m_0$ is the Kane matrix element, and m_0 is the free electron mass. The wave function Ψ_s has to satisfy the following equation:

$$|V|^2\hat{p}^2\Psi_s + \left[(E_g/2)^2 - E^2\right]\Psi_s + \frac{\hbar^2|V|^2}{2E+E_g}\nabla E_g(r)\nabla\Psi_s = 0. \tag{6}$$

For semiconductor microcrystals having the form of a sphere with radius a, $E_g(r)$ is given by:

$$E(r) = \begin{cases} E_g^s, & r < a, \\ E_g^g, & r > a. \end{cases} \tag{7}$$

Taking into account the spherical symmetry of the investigated system we will find the solution of eq. (6) in the form of spherical waves:

$$\Psi_{s,l} = f_l(r)Y_{l,m}(\Omega), \tag{8}$$

where $Y_{l,m}$ are the normalized spherical functions. From eqs. (7) and (8) we obtain the following equation for the radial wave function $f_l(r)$:

$$\frac{1}{r^2}\left[\frac{\partial}{\partial r}r^2\frac{\partial}{\partial r} - \frac{l(l+1)}{r^2}\right]f_l(r) + \frac{1}{\hbar^2|V|^2}\left[E^2 - (E_g/2)^2\right]f_l(r) = 0. \tag{9}$$

The intraspherical $f_l^<(r)$ $(r < a)$ and interspherical $f_l^>(r)$ $(r > a)$ solutions of that equation have to satisfy the boundary conditions

$$f_l^<(a) = f_l^>(a), \tag{10a}$$

$$\frac{1}{E+E_g^s/2}\frac{\partial f_l^<(a)}{\partial r} = \frac{1}{E+E_g^g/2}\frac{\partial f_l^>(a)}{\partial r}. \tag{10b}$$

For the electron states bound in the microcrystal the solutions to eq. (9) satisfying the boundary conditions have the form:

$$f_l(r) = \begin{cases} A_l j_l(\kappa_s r), & r < a \\ A_l\dfrac{j_l(\kappa_s a)}{K_l(\kappa_g a)}K_l(\kappa_g r), & r > a \end{cases} \tag{11}$$

where j_l is a spherical Bessel function, and K_l is connected to a modified Bessel function $K_{l+1/2}$ by the relation: $K_l(z) = = \sqrt{\pi/2z}\,\mathrm{K}_{l+1/2}(z)$ [18]. A_l is the normalization constant and

$$\kappa_g^2 = \frac{1}{\hbar^2|V|^2}\left[(E_g^g/2)^2 - E^2\right], \qquad \kappa_s^2 = \frac{1}{\hbar^2|V|^2}\left[E^2 - (E_g^s/2)^2\right]. \tag{12}$$

Substituting solution (11) in the boundary condition (10) we obtain an equation for determining the electron energy levels:

$$\frac{\partial}{\partial r}\ln\left[j_l(\kappa_s r)\right]\Big|_{r=a} = \frac{E + E_g^s/2}{E + E_g^g/2}\frac{\partial}{\partial r}\ln\left[K_l(\kappa_g r)\right]\Big|_{r=a}. \tag{13}$$

For further calculations it is necessary to have the wave function of the lowest size-quantization level ($l = 0$). It has the following evident form:

$$\Psi_i^{(e)} = \begin{pmatrix} Y_{0,0} f_0(r) \\ \frac{\alpha}{\sqrt{3}} Y_{1,-1}\, \partial f_0/\partial r \\ -\frac{\alpha}{\sqrt{3}} Y_{1,0}\, \partial f_0/\partial r \\ \frac{\alpha}{\sqrt{3}} Y_{1,1}\, \partial f_0/\partial r \end{pmatrix}, \qquad \alpha_{s,g} = \frac{-i\hbar V}{E_0 + E_g^{s,g}/2}, \tag{14}$$

where $f_0(r)$ is given by expressions (11) and (12), E_0 is the energy of the size-quantized electron ground state which is determined from eq. (13). The normalization constant A_0 is:

$$A_0^2 = \frac{E_0 + E_g^s/2}{E_0 a^3}(\kappa_s a)^2 X(\kappa_s, \kappa_g),$$

$$X(\kappa_s, \kappa_g) = \left(1 - \frac{\sin(2\kappa_s a)}{2\kappa_s a} + \frac{\sin^2(\kappa_s a)}{\kappa_g a}\frac{E_g^s + 2E}{E_g^g + 2E}\right)^{-1}. \tag{15}$$

Furthermore, to take into account the electron scattering at the semiconductor/glass heterointerface we write down an analytical form of a free electron wave function:

$$\psi_{l,m}(k, r) = \begin{cases} \psi_<(k_s, l, m; r), & r < a, \\ \psi_>(k_g, l, m; r), & r > a, \end{cases} \tag{16}$$

where

$$\psi_<(k_s, l, m; r) = A_l^f \begin{pmatrix} j_l(k_s r) Y_{l,m} \\ k_s\alpha_s\left[\sqrt{\frac{(l-m+2)(l-m+1)}{2(2l+3)(2l+1)}}\, j_{l+1}Y_{l+1,m-1} + \sqrt{\frac{(l+m)(l+m-1)}{2(2l+1)(2l-1)}}\, j_{l-1}Y_{l-1,m-1}\right] \\ k_s\alpha_s\left[\sqrt{\frac{(l+m+1)(l-m+1)}{(2l+3)(2l+1)}}\, j_{l+1}Y_{l+1,m} - \sqrt{\frac{(l+m)(l-m)}{(2l+1)(2l-1)}}\, j_{l-1}Y_{l-1,m}\right] \\ k_s\alpha_s\left[\sqrt{\frac{(l+m+2)(l+m+1)}{2(2l+3)(2l+1)}}\, j_{l+1}Y_{l+1,m+1} + \sqrt{\frac{(l-m)(l-m+1)}{2(2l+1)(2l-1)}}\, j_{l-1}Y_{l-1,m+1}\right] \end{pmatrix}. \tag{17}$$

Here $k_s^2 = [E_f^2 - (E_g^s/2)^2]/\hbar^2 |V|^2$, E_f is the energy of a free electron and the coefficients α are

$$\alpha_{s,g}(E_f) = -i\hbar V/(E_f + E_g^{s,g}/2). \tag{18}$$

The wave function $\psi_>(k_g, l, m; r)$ is obtained by replacement in eq. (17) of k_s^2 by $k_g^2 = [E_f^2 - (E_g^g/2)^2]/\hbar^2 |V|^2$; of α_s by α_g, and of all spherical Bessel functions $j_p(k_s r)$ by the following expressions:

$$j_p(k_s r) \Rightarrow k_g^2 a^2\left[\Delta_+ j_p(k_g r) + \Delta_- y_p(k_g r)\right], \tag{19}$$

where y_p are spherical Bessel functions of the second kind [18].

$$\Delta_+(p, k_g) = \left[j_p(k_s a) y_p'(k_g a) - (k_s/k_g\gamma) j_p'(k_s a) y_p(k_g a) \right],$$
$$\Delta_-(p, k_g) = \left[(k_s/k_g\gamma) j_p(k_g a) j_p'(k_s a) - j_p(k_s a) j_p'(k_g a) \right], \tag{20}$$

and $\gamma = (E_f + E_g^s/2)/(E_f + E_g^g/2)$. The normalization coefficient A_l^f is determined in accordance with the usual normalization method for the spherically symmetric wave functions:

$$\int \psi_{l,m}^*(k, r) \psi_{l',m'}(k', r) r^2 \, dr \, d\Omega = \delta_{l',l} \delta_{m',m} \delta(k - k'). \tag{21}$$

As a result A_l^f is

$$|A_l^f|^2 = \frac{1}{\pi} \frac{(1 + E_g^g/2E_f)}{a^4 k_g^2 \left[\Delta_+^2(1, k_g) + \Delta_-^2(1, k_g) \right]}. \tag{22}$$

For the calculation of the rate of Auger processes it is necessary to find the form of the hole wave function $\psi_h(r)$. In the investigated phenomena the lowest optically active states of the hole play the main role. In these states the hole energy is mainly due to the heavy hole effective mass m_h and is much less than the height of the barrier at the microcrystal boundary. The hole wave function vanishes on the interface if the barrier has infinite height: $\psi_h(r = a) = 0$. On the other hand the condition $m_h \gg m_e$ (m_e is the electron mass) permits us to neglect the nonparabolicity of the hole energy spectrum and to use a three-band Luttinger model [19] to describe the hole quantization. In this case we neglect the terms of order $(m_e/m_h) \ll 1$ in the overlap integrals of electron and hole wave functions.

In a spherical potential the hole states are characterized by the total momentum J and its projection M. In the framework of the three-band Luttinger model the wave functions of these states can be represented in the form [20]:

$$\psi_h = \psi_{J,M} = \sum_{l=J-1}^{J+1} R_l(r) \sum_{m=-1}^{m=+1} Y_{l,M,m} u_m, \tag{23}$$

where $Y_{l,M,m}$ are the components of the spherical vector $\mathbf{Y}_{l,M}$ [21] and $R_l(r)$ are the radial wave functions. For each value of J, M there are two solutions with different parity. As can be shown the ground state of the hole in a quantum well has $J = 1$. Therefore, we write down the wave function of one of the even* optical-active and Auger-active states ($J = 1$, $M = 0, \mp 1$) which is necessary for further calculations:

$$\psi_{J=1,M=0}(r) = \begin{pmatrix} 0 \\ 0 \\ Y_{0,0} \\ 0 \end{pmatrix} R_0(r) - \begin{pmatrix} 0 \\ \sqrt{3/10}\, Y_{2,-1} \\ \sqrt{2/5}\, Y_{2,0} \\ \sqrt{3/10}\, Y_{2,1} \end{pmatrix} R_2(r). \tag{24}$$

The zeros in the upper line correspond to the neglect of the conduction band contribution to the heavy

* The analysis of the selection rules shows that the odd state of a hole with $J = 1$ does not give the contribution to the Auger processes and the optical transitions in the dipole approximation are forbidden.

hole wave function under the condition $m_e/m_h \ll 1$. The radial wave functions R_0, R_2 satisfy the equations

$$-\left(\frac{1}{m_l}+\frac{2}{m_h}\right)\frac{1}{r^2}\left(\frac{d^2}{dr^2}+\frac{2d}{r\,dr}\right)R_0+2\left(\frac{1}{m_l}-\frac{1}{m_h}\right)\left(\frac{d^2}{dr^2}+\frac{5d}{r\,dr}+\frac{2}{r^2}\right)R_2=(6/\hbar^2)(E_h-U(r))R_0,$$
$$2\left(\frac{1}{m_l}-\frac{1}{m_h}\right)\left(\frac{d^2}{dr^2}-\frac{d}{r\,dr}\right)R_0-\left(\frac{2}{m_l}-\frac{1}{m_h}\right)\left(\frac{d^2}{dr^2}+\frac{2d}{r\,dr}-\frac{6}{r^2}\right)R_2=(6/\hbar^2)(E_h-U(r))R_2, \tag{25}$$

where m_l is the light hole effective mass, $U(r)$ is the spherically symmetric potential acting on the hole. In the simplest case of "strong" size quantization we neglect the Coulomb interparticle interaction and obtain for radial wave functions

$$R_0=C_0a^{-3/2}[j_0(\phi_2 r/a)-j_0(\phi_2)],$$
$$R_2=-\tfrac{1}{2}C_0a^{-3/2}j_2(\phi_2 r/2), \tag{26}$$

where $\phi_2\approx 5.76$ is the first root of the Bessel function $j_2(x)$, $|C_0|^2\approx 48.5$ is determined from the normalization condition. In this approximation the energy of the hole quantum size level is $E_h=\hbar^2\phi_2^2/2m_ha^2$.

4. The Auger ionization rate of quantum drops

Auger disintegration is a many-electron process in which the energy of the electron–hole pair annihilation is transferred to one electron. In the case when this energy is larger than the barrier height the electron ejects into the glass and ionization of the microcrystal takes place. We will consider the probability of Auger disintegration when both electrons and both holes are situated on the lowest quantum size level. If we neglect the Coulomb interaction the initial antisymmetric wave function of the two-electron state may be written in the form:

$$\langle\psi^i|=\psi_i^{(e)}(\boldsymbol{r}_1)\psi_i^{(e)}(\boldsymbol{r}_2)\frac{\alpha(1)\beta(2)-\alpha(2)\beta(1)}{\sqrt{2}}, \tag{27}$$

where ψ_i^e is the wave function of the electron ground state (see eq. (14)), α and β are the components of the spin wave function with projection $\pm\frac{1}{2}$. As a result of the Auger process one of the electrons annihilates with the hole and the other one ejects into the continuous spectrum. The antisymmetric wave function of such final state has the form:

$$|\psi^f_{k,l,m}\rangle=\frac{\psi_{J=1,M}(\boldsymbol{r}_1)\psi_{l,m}(k,\boldsymbol{r}_2)+\psi_{J=1,M}(\boldsymbol{r}_2)\psi_{l,m}(k,\boldsymbol{r}_1)}{\sqrt{2}}\,\frac{\alpha(1)\beta(2)-\alpha(2)\beta(1)}{\sqrt{2}}. \tag{28}$$

Here we take into account that the Coulomb interaction leading to the Auger disintegration cannot change the spin state of the system. Since the initial and final wave functions are known we calculate the Auger ionization rate of microcrystals τ_A to be

$$\frac{1}{\tau_A}=\frac{2\pi}{\hbar}\sum_{l,m,M}\int|\langle\psi^i|v(\boldsymbol{r}_1,\boldsymbol{r}_2)|\psi^f_{k,l,m}\rangle|^2\delta(E_i-E_f)\,dk, \tag{29}$$

where the sum is over the quantum numbers of spherically symmetric final states of the electron, l, m, k, and the hole M [22], $v(\boldsymbol{r}_1,\boldsymbol{r}_2)=e^2/\kappa|\boldsymbol{r}_1-\boldsymbol{r}_2|$ is the Coulomb repulsive potential for the electrons, κ is the dielectric coefficient. The angle integration in eq. (29) gives the nonzero matrix elements only for final

states with $l=1$ and $m=M$. Such "selection rules" for transitions are due to the conservation of total moment. We obtain

$$\frac{1}{\tau_A}=\frac{2\pi}{\hbar}2\left|\langle\psi^i\,|\,v(r_1,\,r_2)|\psi^f_{k_g,l=1,m=M=0}\rangle\right|^2\left(\frac{\partial E(k)}{\partial k}\bigg|_{k=k_g}\right)^{-1}, \tag{30}$$

where $E(k_g)$ is the dispersion law for a free electron in glass, and k_g is the quasi-momentum of the ejected electron. The matrix element in eq. (29) is independent of M because of the spherical symmetry. Therefore, we calculate only the matrix element for the state with $M=0$, and the factor 2 in eq. (30) takes into account the probability of annihilation of the electron with two holes of the initial state.

The calculation of the matrix element in eq. (30) is carried out by the standard technique of the multipole expansion of the Coulomb potential. Introducing dimensionless variables of integration $x'=r_1/a$ and $x=r_2/a$ we obtain the Auger ionization rate by the cumbersome but trivial calculation:

$$\frac{1}{\tau_A}=\frac{8|C_0|^2}{27}\chi^2(\kappa_s,\,\kappa_g)\frac{\left[1-\left(\frac{E_g^s}{2E_0}\right)^2\right]\left(1+\frac{E_g^g}{2E_f}\right)}{\Delta_+^2(1,\,k_g)+\Delta_-^2(1,\,k_g)}\frac{(\kappa_s a)^4}{(k_g a)^3}\left(\frac{e^2}{\hbar|V|\kappa}\right)^2\frac{E_f}{\hbar}|M_A|^2, \tag{31}$$

where matrix element M_A is the sum of two integrals

$$M_A=J_<(k_s,\,\kappa_s)+\frac{j_0(\kappa_s a)}{K_0(\kappa_g a)}\eta(\kappa_s a)(k_g a)^2 J_>(k_g,\,\kappa_g). \tag{32}$$

In the first one, $J_<$, the integration is carried out over the volume of the microcrystal:

$$\begin{aligned}J_<(k_s,\,\kappa_s)=&\iint_{|x|,|x'|<1}\mathrm{d}x\,\mathrm{d}x'x^2x'^2j_h(x)j_1(\kappa_s a x)\frac{x_<}{x_>^2}\\&\times\left\{j_1(k_s a x')j_0(\kappa_s a x')-(k_s\kappa_s/3)\alpha_s(E_f)\alpha_s(E_0)\left[j_0(k_s a x')\right.\right.\\&\left.\left.+2j_2(k_s a x')\right]j_1(\kappa_s a x')\right\},\end{aligned} \tag{33}$$

where $x_>=\max\{x,\,x'\}$, $x_<=\min\{x,\,x'\}$. In the other one it is carried out over the volume of the glass matrix surrounding of the microcrystal:

$$\begin{aligned}J_>(k_g,\,\kappa_g)=&\int_1^\infty\mathrm{d}x\left\{K_0(\kappa_g a x)\left[\Delta_+(1,\,k_g)j_1(k_g a x)+\Delta_-(1,\,k_g)y_1(k_g a x)\right]\right.\\&-(k_g\kappa_g/3)\alpha_g^*(E_f)\alpha_g(E_0)K_1(\kappa_g a x)\left[2\Delta_+(2,\,k_g)j_2(k_g a x)+\Delta_+(0,\,k_g)j_0(k_g a x)\right.\\&\left.\left.+\Delta_-(2,\,k_g)y_2(k_g a x)+2\Delta_-(0,\,k_g)y_0(k_g a x)\right]\right\},\end{aligned} \tag{34}$$

$$\eta(\kappa_s a)=\int_0^1\mathrm{d}x'x'^3j_h(x')j_1(\kappa_s a x'), \tag{35}$$

where $j_h(x)=j_0(\phi_2 x)-j_2(\phi_2 x)-j_0(\phi_2)$. In expressions (33) and (34) the range of integration is divided into two regions.

The expression for the probability of the Auger ionization (31) has a rather complicated structure. To reveal the physical nature of the Auger disintegration processes we consider first the case when the ejected electrons have large final momenta $k_g a\gg 1$, as is the case for $\Delta E=|E_g^g-E_g^s|\ll E_g^s$. At this condition $\epsilon_0\ll E_g^s$, where $\epsilon_0=\hbar^2/2m_e a^2$ is a typical energy scale for the size-quantized electron, $k_g\approx k_s$ since $\Delta E/E_g\ll 1$ and eq. (20) reduces to $\Delta_-(1,\,k_g)\Rightarrow 0$, $\Delta_+(1,\,k_g)\Rightarrow 1/(k_g a)^2$. The energy of an electron ejected from the microcrystal is $E_f\approx 3/2E_g^s$. The above choice of heterostructure parameters leads to

$\alpha_s^2(E_0)/a^2 \approx \alpha_g^2(E_0)/a^2 \approx \hbar^2 |V|^2/(aE_g^s)^2 \approx \epsilon_0/E_g^s \ll 1$ and $X \approx 1$. Substituting all these values into expression (31) for the Auger disintegration probability we obtain

$$\frac{1}{\tau_A} = \frac{64\sqrt{2}}{27} |C_0|^2 \pi^5 \left(\frac{e^2}{\hbar |V| \kappa}\right)^2 \left(\frac{\epsilon_q}{E_g^s}\right)^{1/2} \frac{E_g^s}{\hbar} |M_A|^2, \tag{36}$$

where $\epsilon_q = \hbar^2\pi^2/2m_e a^2$ is the energy of an electron ground state in a well with infinitely high walls. Under the condition $k_{s,g}^{-1} \ll a$ the integrand in M_A can be written as the product of a rapidly oscillating function and a smooth function. The integrals then can be expanded as a power series in the small parameter $(ak_{g,s})^{-1} \ll 1$, the coefficients of which are determined by the special points of the smooth function [23]. In our case these points are $x = 0$ and $x = 1$ (the boundaries of a microcrystal). It can be shown that the largest term in this power series is determined by the region of the special point $x = 1$. The coefficient of $(ak_{g,s})^{-2}$ and $(ak_{g,s})^{-3}$ vanish because of the requirements of continuity of the wave function and its derivative at the microcrystal boundaries. The first nonzero term is $(ak_{g,s})^{-4}$. The region of the other special point $x = 0$ contributes to the terms of higher order in $(ak_{g,s})^{-1}$. This calculation gives for the matrix element M_A

$$M_A = \eta(\kappa_s a) \frac{\sin(k_g a) \sin(\kappa_s a)}{\kappa_s a (k_s a)^4} \times \left\{ \left[3(\kappa_s a + 1)(\kappa_g a + 1) + (\kappa_g a)^2 - (\kappa_s a)^2 \right] + \left[\frac{(\kappa_g a)^2 + (\kappa_s a)^2}{3} \right] \right\}. \tag{37}$$

Here, the first and second items in braces correspond to the contribution from the conduction and valence band. It is seen that these contributions may become of the same order of magnitude at a large value of $(ak_{g,s}) \gg 1$. If the energy of the size quantization ϵ_q is much smaller than the depth of the well $\Delta = (E_g^g - E_g^s)/2$ ($\epsilon_q \ll \Delta$) expression (36) is great simplified. Then $\kappa_s a = \pi(1 - 1/\kappa_g a)$ and $\kappa_g a \approx (\Delta/\epsilon_0)^{1/2}$. Averaging the fast changing value $\sin^2(k_g a)$ in eq. (36) ($\langle \sin^2(k_g a) \rangle = \frac{1}{2}$) and taking into account that $\eta(\pi) = 2.15 \times 10^{-2}$ we obtain

$$\left\langle \frac{1}{\tau_A} \right\rangle = 1.8 \times 10^{-3} \left(\frac{e^2}{\hbar |V| \kappa}\right)^2 \frac{E_g^s}{\hbar} \left(\frac{\epsilon_q}{E_g^s}\right)^{7/2} \left(\frac{\Delta}{E_g^s}\right). \tag{38}$$

It is seen that the Auger ionization rate decreases as the size of microcrystal grows and follows the law $\langle 1/\tau_A \rangle \sim a^{-7}$. Carrying out the numerical computation we obtain for a semiconductor with CdS energy band parameters, mentioned later

$$\left\langle \frac{1}{\tau_A} \right\rangle = 2.9 \times 10^7 \text{ s}^{-1} \left(\frac{30 \text{ Å}}{a}\right)^7. \tag{39}$$

We want to note that the asymptotic expression (39) is valid only for microcrystals with large enough radius and for quantum structures in which $k_s a \approx k_g a \gg 1$.

The other limit is of interest when the momentum of the electron ejected into glass k_g is much smaller than the typical momentum of the bound electron $\sim a^{-1}$: $k_g a \ll 1$. This is possible under the following condition:

$$E_g^g/2 - 3E_g^s/2 \ll 2\epsilon_q, \tag{40}$$

and can be realized by a special choice of the energy band parameters. In this case, as earlier, $k_s a \gg 1$. At $k_g a \ll 1$ the values entering in eq. (31)–(33) are $E_f \approx 1.5E_g^s \approx E_g^g/2$ and

$$\Delta_+(1, k_g) = \frac{1}{(ak_g)^3} \left[2j_1(k_s a) + k_s a/\gamma \cdot j_1'(k_s a) \right], \qquad \Delta_-(1, k_g) = \tfrac{1}{3} \left[k_s a/\gamma \cdot j_1'(k_s a) - j_1(k_s a) \right]. \tag{41}$$

At $k_g a \ll 1$ the integrand in M_A oscillates fast only within the inner range of the integration ($x < 1$). As a result the main term in the parameter $(k_s a)^{-1} \ll 1$ yields the following expression for $J_<$:

$$J_< = -\frac{1}{(\kappa_s a)(k_s a)} j_0(k_s a) j_0(\kappa_s a) \eta(\kappa_s a). \tag{42}$$

The condition $k_g a \ll 1$ permits us to neglect the contribution of the valence band states to $J_>$. Furthermore, the value of $J_>$ is determined only in the neighborhood of the microcrystal boundaries, since $\kappa_s \gg 1/a$. As a result, using eq. (41) we obtain for $J_>$:

$$J_> = \frac{1}{(k_g a)^2} j_1(k_s a) K_0(\kappa_g a) \eta(\kappa_s a). \tag{43}$$

From eqs. (41) and (42) it follows:

$$M_A = \left[-\frac{1}{k_s a} j_0(k_s a) + j_1(k_s a) \right] j_0(\kappa_s a) \eta(\pi) \approx -\frac{\cos(k_s a)}{(\kappa_g a)(k_s a)} \eta(\pi). \tag{44}$$

In obtaining eq. (44) we use the relationship $\kappa_s a \approx \pi(1 - 1/\kappa_g a)$. Substituting eq. (44) into eq. (31) and taking into account that $X \approx 1$ we find

$$\frac{1}{\tau_A} \approx \tfrac{32}{91} |C_0|^2 \eta^2(\pi) \left(\frac{e^2}{\hbar |V| \kappa} \right)^2 \left(\frac{\epsilon_q}{E_g^s} \right)^3 \frac{E_g^s}{\hbar}$$

$$\times \cos^2(k_s a) \frac{(k_g a)^3}{(\sin(k_s a) + 2\cos(k_s a)/(3k_s a))^2 + \left((k_g a)^3 \sin(k_s a) \right)^2 / 9}. \tag{45}$$

It is seen from eq. (45) that the probability of Auger disintegration is a strongly oscillating function. The proportionality of $1/\tau_A$ to $\cos^2(k_s a)$ is connected with quantum interference of electron states taking part in Auger disintegration. As in the case of $k_s a \gg 1$ and $k_g a \gg 1$, it results in the vanishing of the matrix element M_A at some values of $k_s a$. Of more interest is the increase of the Auger disintegration rate which is due to resonance effects and which is described by the last factor in eq. (45). The value of this factor changes, over a wide range, from $(k_g a)^3$ to $(k_g a)^{-3}$. Such a resonance increase of $1/\tau_A$ occurs when $\sin(k_s a) + \frac{2}{3} \cos(k_s a)/(k_s a) = 0$*, corresponding to the merging of the electron quantum-size level with $l = 1$ into the continuous spectrum. As is seen from eq. (45) the width of such resonance is $\Gamma \sim (k_g a)^3$. The dependence of Γ on the free electron momentum k_g is typical for resonance scattering of p-waves [22].

Averaging the oscillations of the Auger disintegration probability gives a smooth dependence $\langle 1/\tau_A \rangle$ on the radius of a microcrystal a:

$$\left\langle \frac{1}{\tau_A} \right\rangle = \frac{16\sqrt{2}\pi}{9} |C_0|^2 \eta^2(\pi) \left(\frac{e^2}{\hbar |V| \kappa} \right)^2 \left(\frac{\epsilon_q}{E_g^s} \right)^{5/2} \frac{E_g^s}{\hbar}, \tag{46}$$

which behaves as $\langle 1/\tau_A \rangle \sim a^{-5}$. In that case the rate of Auger disintegration as a result of the resonance effect is substantially larger than it is in the case of large momentum of the ejected electron ($k_g a \gg 1$).

The band parameters of the CdS microcrystals investigated fall into the intermediate range between two limiting cases. Therefore, describing the experimental results it is necessary to use the full expression for the probability of Auger disintegration (31). In fig. 5 we show the dependence of the Auger ionization probability on the microcrystal radius. The computation was carried out for the CdS microcrystal

* This equation coincides with dispersion relationship (13) under the conditions: $k_s a \gg 1$, $E_g^g = 3E_g^s$.

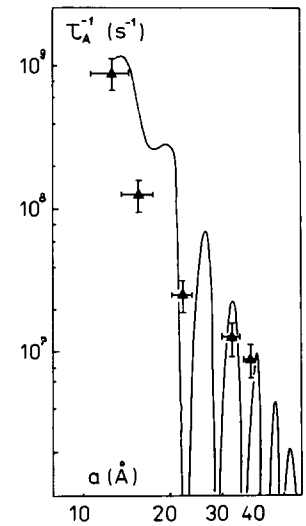

Fig. 5. The theoretical dependence of the Auger ionization probability of CdS microcrystals on their radius a. The crosses show the experimental data.

parameters: $E_g^s = 2.58$ eV, $m_e = E_g^s/2|V|^2 = 0.2m_0$ and $e^2/\hbar|V|\kappa = 0.15$. The value of an effective energy gap of glass $E_g^g = 7.02$ eV was obtained from direct experimental photoionization data on CdS microcrystals dispersed in glass [12].

As can be seen from fig. 5 the probability of Auger disintegration has a strong oscillatory character. The computed maxima of $1/\tau_A$ correspond to microcrystals for which the $l = 1$ quantum-size levels either cross the boundary of the continuous spectrum or are close to it. This situation is in qualitative agreement with the effect of the resonance Auger disintegration considered analytically in the limit $k_g a \ll 1$. Minimal values of $1/\tau_A$ are due to the vanishing of the matrix element M_A, caused by the quantum mechanical interference of the electron wave functions talking part in the Auger process.

In real structures the oscillations $1/\tau_A$ are averaged out. This is caused by numerous reasons, such as disordering of glass matrix, dispersion of the microcrystal sizes and shapes, and fluctuations of the semiconductor/glass band offset. We took into account these effects when we carried out the averaging of eq. (31) to obtain eqs. (38) and (46) at large values of the ejected electron momentum ($k_s a \gg 1$). Nevertheless, the possibility exists of observing quantum oscillations in $1/\tau_A$ when the momenta of the electrons $k_{s,g}$ taking part in the Auger process are comparable to the inverse size of a microcrystal ($k_{s,g} a \sim 1$).

5. Discussion of the results

In this part we compare the experimental dependences of ionization time τ_i on the absorbed power P (see fig. 3) and average microcrystal radius $\bar{a}$ (see fig. 4) with our theoretical calculation of the probability of the Auger disintegration τ_A^{-1}. So long as τ_A is independent of P, τ_i^{-1} has to be proportional to P^ν with $\nu = 2$, as follows from section 2. Such a degradation process is evidence for a two-photon mechanism. In our model τ_i^{-1} is proportional to the steady state value of the fraction of the microcrystals containing two nonequilibrium electron–hole pairs $(W_{01}\tau_0^{(1)})(W_{12}\tau_0^{(2)})$. Though this fraction is small at low excitation intensity, Auger ionization leading to degradation is possible only in these microcrystals. It is clear that

this kind of dependence is not connected with the size of microcrystals. As was mentioned in section 2, the experimental dependence yields $\nu = 1.8 \pm 0.3$. This value agrees with the prediction of the Auger ionization model ($\nu = 2$) within the experimental accuracy. The observed systematic deviation to a smaller value of ν may be connected to the method of measurement of the luminescence degradation, which was obtained from the time dependent quantum efficiency of the interimpurity luminescence. It is well known that the bands due to donor–acceptor pair radiative recombination in bulk semiconductor shift to shorter wavelengths with increasing excitation intensity. The same effect was observed in semiconductor microcrystals [7]. Here, however, the dependence of the shift of the luminescence band maxima on I is complicated by the fact that there exists a dispersion in the size of microcrystals contained in the sample. Therefore, the observed long wavelength edge of the interimpurity band is due to the larger microcrystals, whereas the short wavelength edge is formed by the smaller microcrystals. With increasing the excitation level at fixed frequency of the emitted light we detect luminescence from microcrystals of larger and larger size a. The probability of Auger ionization decreases as a grows, leading to some decrease in ν.

The experimental dependence of the ionization time τ_i on the average microcrystal radius $\bar{a}$ was approximated as $\tau_i \sim (\bar{a})^{4.5}$ at fixed P (see fig. 2). This dependence is weaker than the theoretical one $\tau_i \sim \tau_A \sim a^5$ (see eq. (46)). It is necessary to note that the real parameters of our structures do not permit the use of the asymptotic expression (46). This means that dependence of τ_i on $\bar{a}$ cannot be approximated by the power function and has a more complicated form (see fig. 5). It is seen in fig. 4 that the experimental dependence of $\tau_i(\bar{a})$ is actually not a power of a. Therefore, it is necessary to directly compare the experimental data to the results of a numerical calculation of $\tau_A(a)$ from eq. (31). We obtained the experimental values of $\tau_A(\bar{a})$ from the experimentally observed $\tau_i(\bar{a})$ by using eq. (3). To do this it is necessary to estimate the steady state fraction of microcrystals containing two electron–hole pairs. Estimating that as the square of the steady state fraction of a singly excited microcrystal $W_{01}\tau_0$, we obtain in our experiment that $\tau_A = (W_{01}\tau_0^{(1)})^2\tau_i \approx 10^{-10}\tau_i$ (the value $W_{01}\tau_0(1) \sim 10^{-5}$ was estimated from the absorbed power).

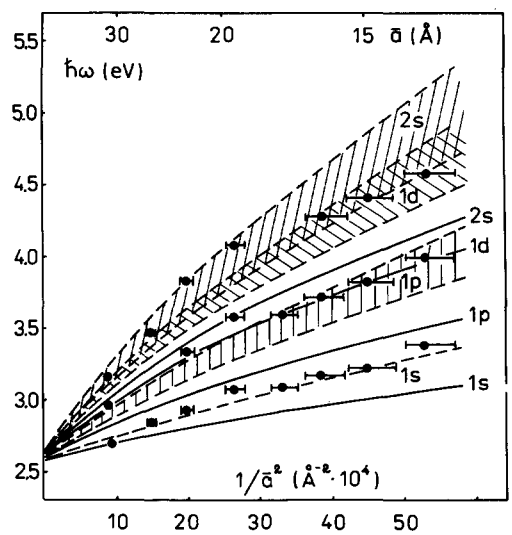

Fig. 6. The dependence of maximum positions in interband absorption spectra on CdS microcrystal size. Experimental data are shown by the horizontal segments which lengths reflect the accuracy of the measurements of the average microcrystal radius $\bar{a}$. Dashed lines show the theoretical dependences of transition energies to the lowest electron quantum-size level (1s, 1p, 1d, 2s) on a. The shading shows the overlap region of these transitions. The solid lines displays the dependences of the lowest electron quantum-size level on a, calculated in the framework of the Kane model.

The probability of Auger disintegration τ_A^{-1} obtained in such a way is shown in fig. 5. It is seen that the experimental data are in good agreement with the theoretical dependence. However, a more detailed analysis of the experimental data is difficult to make. There are many reasons for that, such as the dispersion of microcrystal size, disordering of the glass matrix structure, and fluctuations of relative band offset in the semiconductor/glass heterostructure. All of them lead to the smoothing of quantum oscillations. It seems to us that oscillations of τ_A^{-1} might possibly be observed experimentally in samples containing small size microcrystals with low dispersion.

Let us discuss the applicability of the Kane model to the description of energy and wave function of semiconductor/glass heterostructure electron states. This problem includes the question of boundary conditions, taking into account the different character of atomic (Bloch) functions in semiconductors and in glass. It is especially important since the abrupt heterointerface which is shown in section 4 significantly increases the rate of Auger processes. Nevertheless, the Kane model gives quantitative and qualitative agreement with experiment not only for the times of Auger ionization but for the energy dependence of quantum-size electron levels on the size of microcrystals. These dependences obtained from eq. (13) are shown by solid lines in fig. 6. It also gives the experimental energies of interband transitions to the quantum-size electron levels. The dashed lines here show the theoretical dependence of the total energy of the optical transitions on a, obtained on the assumption of "strong" size quantization of holes [2]. The energies of the quantum-size hole levels are calculated taking into account the six-fold degeneracy of the valence band (see section 3). In that case the selection rules permit the transition from some quantum-size hole levels and the dashed lines show the two strongest transitions from them to every quantum-size electron level: 1p, 1d, 2s. The regions between these lines are shaded since the dispersion of the microcrystal size leads to substantial broadening of every transition, resulting in their overlap. It is seen that experimental and theoretical results are in good agreement. The experimentally observed and theoretically predicted deviation of behavior of the optical transition energy from the $1/a^2$ law is mainly due to the nonparabolicity of the conduction band. The calculation carried out shows that the finite depth of the quantum well does not play a significant role in this effect.

The authors are grateful to M.E. Raikh, A.E. Cherednichenko and S.A. Fillippova for valuable discussion and help.

References

[1] A.I. Ekimov and A.A. Onushchenko, Sov. Phys. Semicond. 16 (1982) 775.
[2] Al.L. Efros and A.L. Efros, Sov. Phys. Semicond. 16 (1982) 772.
[3] R. Rosetty, S. Nakahara and L.E. Brus, J. Chem. Phys. 79 (1983) 1086.
[4] D.S. Chemla and D.A.B. Miller, J. Opt. Soc. Amer. B 2 (1985) 1155.
[5] Y. Kayanuma, Phys. Rev. B 38 (1989) 9797.
[6] A.I. Ekimov, Al.L. Efros and A.A. Onushchenko, Solid State Commun. 56 (1985) 921.
[7] A.I. Ekimov, I.A. Kudriavtsev, M.G. Ivanov and Al.L. Efros, Sov. Phys. Solid State 31 (1989) 1385.
[8] G.L. Olbright and N. Peyghambarian, Appl. Phys. Lett. 48 (1986) 1148.
[9] U.V. Vandichev, V.S. Dneprovskii, A.I. Ekimov, D.K. Okorokov, L.B. Popova and Al.L. Efros, JETP Lett. 46 (1987) 495.
[10] P. Roussignol, D. Ricard, J. Lukasik and G.C. Flitzanis, J. Opt. Soc. Amer. B 4 (1987) 5.
[11] A.I. Ekimov, Al.L. Efros, Phys. Stat. Sol. (b) 150 (1988) 627.
[12] V.I. Grabovskis, Y.Y. Dzenis, A.I. Ekimov, I.A. Kudriavtsev and M.N. Tolstoii, Sov. Phys. Solid State 31 (1989) 149.
[13] V.V. Golubkov, A.I. Ekimov, A.A. Onushchenko and V.A. Tsekhomskii, Fiz. Khim. Stekla 7 (1981) 397.
[14] A.I. Ekimov and A.A. Onushchenko, JETP Lett. 40 (1984) 1136.
[15] B.L. Gel'mont, V.A. Kharchenko and I.N. Yasievich, Sov. Phys. Solid State 29 (1987) 1355.
[16] E.O. Kane, J. Phys. Chem. Sol. 1 (1956) 249.
[17] R.A. Suris, Fiz. Tekhn. Poluprov. 20 (1986) 2008.

[18] M. Abramowiz and I.A. Stegun, eds., Handbook of Mathematical Functions with Graphs and Mathematical Tables (Dover, New York, 1964).
[19] J.M. Luttinger, Phys. Rev. 102 (1956) 1030.
[20] B.L. Gel'mont and M.I. D'yakonov, Sov. Phys. Semicond. 5 (1972) 1905.
[21] A.I. Akhiezer and V.B. Berestetskii, Quantum Electrodynamics (Interscience, New York, 1965).
[22] L.D. Landau and E.M. Lifchitz, Quantum Mechanics, (Pergamon, Oxford, 1974).
[23] A.B. Migdal, The qualitative methods of quantum theory (Nauka, Moskva, 1975).